Journal of Orthopaedic Translation 48 (2024) 232–243

Contents lists available at ScienceDirect

Journal of Orthopaedic Translation

journal homepage: www.journals.elsevier.com/journal-of-orthopaedic-translation

Original Article

Biomarkers for hypertrophic chondrocyte differentiation are associated with spatial cellular organisation and suggest endochondral ossification-like processes in osteoarthritic cartilage: An exploratory study

Julius Michael Wolfgart [a,g], Lea Cathrine Grötzner [a,b], Sascha Hemayatkar-Fink [a,c], Maik Schwitalle [d], Florian Christof Bonnaire [a,e], Martina Feierabend [a,f,*], Marina Danalache [a], Ulf Krister Hofmann [a,g]

[a] Laboratory of Cell Biology, Department of Orthopaedic Surgery University Hospital of Tübingen, Waldhörnlestraße 22, D-72072, Tübingen, Germany
[b] Medical Faculty of the University of Tübingen, D-72076, Tübingen, Germany
[c] Department of Trauma and Orthopaedic Surgery and Sports Medicine, Kreiskliniken Reutlingen, Steinenbergstraße 31, D-72764, Reutlingen, Germany
[d] Winghofer Medicum, Röntgenstraße 38, D-72108, Rottenburg am Neckar, Germany
[e] Institute for Diagnostic and Interventional Radiology, Kreiskliniken Reutlingen, Steinenbergstraße 31, D-72764, Reutlingen, Germany
[f] Metabolic Reconstruction and Flux Modelling, Institue for Plant Sciences, University of Cologne, Germany
[g] Department of Orthopaedic, Trauma, and Reconstructive Surgery, Division of Arthroplasty, RWTH Aachen University Hospital, Pauwelsstraße 30, D-52074, Aachen, Germany

ARTICLE INFO

Keywords:
Angiogenesis
Articular cartilage
Endochondral ossification
Hypertrophic differentiation
Osteoarthritis
Spatial chondrocyte organization

ABSTRACT

Background: In healthy articular cartilage, chondrocytes are found along arcades of collagen fibers as Single Strings. With onset of cartilage degeneration this pattern changes to Double Strings. In the course of osteoarthritis Small Clusters, and finally Big Clusters form. In highly degenerated articular cartilage, another poorly understood pattern is found where chondrocyte morphology differs considerably, and the distribution of cells is diffuse. Progression of osteoarthritis is accompanied by key processes such as chondrocyte proliferation, apoptosis, hypertrophic differentiation, inflammation, and angiogenesis. The aim of this exploratory study was to identify biomarkers for these processes in the context of spatial cellular organizational changes in articular cartilage.

Methods: Cartilage explants (n = 166 patients) were sorted according to their predominant cellular pattern. Quantitative or semi-quantitative analysis of 39 biomarkers were performed by multiplex assay (31) or ELISA (8), and qualitative analysis on 12 immunohistochemical markers.

Results: Hypertrophic differentiation (e.g. type-X collagen, osteopontin, osteocalcin and interleukin-6) and angiogenesis were associated with changes in chondrocyte organisation. First changes take place already at the transition from Single Strings to Double Strings. Drastic changes in the appearance of numerous biomarkers are found at the transition from Big Clusters to Diffuse.

Conclusion: Key processes in osteoarthritis and their biomarkers seem to depend on the spatial distribution of chondrocytes in articular cartilage. Abrupt changes in biomarker occurrence were observed between Big Clusters and Diffuse insinuating that the Diffuse pattern is composed of a different cell population or at least a different form of chondrocyte morphology.

The Translational Potential of this Article: In situ identification of the different spatial chondrocyte patterns by fluorescence microscopy has already been established in the recent past. Analysing human in-situ cartilage

Abbreviations: AKT, Serine/threonine-protein kinase; BAD, BCL2 associated agonist of cell death; BC, Big Clusters; BCL2, BCL2 apoptosis regulator; BMP9, Bone morphogenic protein 9; CTLA4, Cytotoxic T-lymphocyte associated protein 4; DIF, Diffuse; DKK1, Dickkopf WNT signaling pathway inhibitor 1; DS, Double Strings; EGF, Epidermal growth factor; FGF1, Fibroblast growth factor 1; FGF2, Fibroblast growth factor 2; FGF23, Fibroblast growth factor 23; HBEGF, Heparin binding EGF like growth factor; HGF, Hepatocyte growth factor; JNK, JUN N-terminal kinase; MIF, Macrophage migration inhibitory factor; PD1, Programmed cell death 1; PECAM1, Platelet endothelial cell adhesion molecule 1; SFAS, Soluble Fas receptor; SFASL, Soluble Fas ligand; SC, Small Clusters; SS, Single Strings; TGF-α, Transforming growth factor alpha; TIM3, T-cell immunoglobulin mucin family member 3; TLR2, Toll-like receptor 2; TNF-α, Tumor necrosis factor alpha; TRAIL, TNF superfamily member 10; VEGF, Vascular endothelial growth factor.

* Corresponding author.
E-mail address: mfeierab@uni-koeln.de (M. Feierabend).

https://doi.org/10.1016/j.jot.2024.08.006
Received 30 June 2023; Received in revised form 27 June 2024; Accepted 6 August 2024

explants rather than isolated OA chondrocytes closes the gap between in vitro and in vivo studies and as such, stretches a big step towards translation of the observed findings. The direct association between tissue biomarker profile and cellular arrangements representing different states of OA sheds new light on the molecular and cellular physiopathology, especially in the context of larger processes such as angiogenesis, cellular proliferation, differentiation, and apoptosis. This also opens an interesting perspective for future investigation of such biomarkers and processes in clinical studies.

1. Introduction

Several key processes have been defined as being characteristic for osteoarthritis (OA), such as cell proliferation [1], apoptosis [2] and differentiation of chondrocytes [3,4], as well as inflammation [5] and angiogenesis [6]. These processes have usually been evaluated as a function of radiographic [7] or macroscopic [8] degeneration of cartilage or based on histologic grading taking into account the wear from the cartilage surface [9]. Thus, the inferences drawn from such studies are based on aspects like matrix degeneration or even subchondral bone modelling as an indirect phenomenon of OA. Recently, a model has been proposed that allows the grading of local cartilage degeneration based on cellular spatial organisation [10,11], which is a parameter that directly addresses the living unit of the cartilage: the chondrocytes. In the femoral condyle, in healthy tissue, chondrocytes are organised as Single Strings (SS). With the onset of OA, a change in the cellular pattern takes place and initially Double Strings (DS) form, followed by Small Clusters (SC), and finally Big Clusters (BC). In end-stage OA, another little understood pattern is described in which the cells do not arrange themselves in any specific way (Diffuse - DIF). These patterns appear to be arranged in a concentric way around cartilage lesions [12]. Spatial chondrocyte organisation as an image-based biomarker has already been shown to strongly correlate with pericellular matrix degradation [13,14] and cartilage elasticity [15-17].

During OA, the morphology of chondrocytes also changes: In SC, but especially in BC, the chondrocytes become larger and appear vesicular, which is described as terminal hypertrophic differentiation [18]. This morphological phenomenon is considered a change in phenotype, which is also characterised by altered protein expression: an increased production could, for example, be shown for type X collagen [19], osteocalcin, and osteopontin [20], which can all be triggered by e.g., interleukin 6 (IL6) through phosphoinositide 3-kinase/serine/threonine-protein kinase (PI3K/AKT) signalling [21,22]. The exact significance and implication of this terminal hypertrophic differentiation has not yet been conclusively clarified. Van der Kraan et al. suggested a connection to the hypertrophic chondrocyte phenotype as it is described for endochondral ossification [23]. Such an altered phenotype and synthesis of proteins contribute to the imbalance of cartilage homeostasis and ultimately cartilage degeneration. Changes in spatial organisation of chondrocytes are an image-morphological correlate of cartilage degeneration at the microscopic level following a defined chronology from SS to DIF [24]. We hypothesised that the presence of proteins associated with hypertrophic chondrocyte differentiation is closely connected to changes in spatial chondrocyte organisation in degenerating cartilage (Hypothesis I).

Angiogenesis in the form of blood vessels sprouting into the cartilage from the subchondral bone is another key feature of OA [25]. Nerve fibres accompanying these blood vessels are one cause of growing pain in the course of the disease [26]. VEGF is a prominent angiogenesis factor that can trigger such processes, and it was the first biomarker discovered in this context [27]. Other angiogenic factors, such as FGF1 and angiopoietin 2, have been poorly studied in osteoarthritic cartilage. We hypothesised that the presence of such biomarkers of angiogenesis also changes as the spatial chondrocyte spatial patterns change (Hypothesis II).

Rolauffs et al. described lesion-associated surface aggregations in cartilage taken near a grade 2 focal lesion [24] that did not match any previously reported organisational patterns [28]. The authors described these patterns as "unorganised" and "diffuse" [14]. To date, little information exists on this pattern; it is unclear whether it occurs as the end stage of a linear progression during cartilage degeneration [24] or if it is the result of immune cell infiltration due to a focal defect [29]. This pattern category differs considerably from the other proposed spatial patterns in at least two aspects: Firstly, the cells are not allocated to one specific pattern, but scattered diffusely in the tissue [24]. Secondly, their morphologic appearance is no longer smooth elliptical, spheroidal, and sometimes swollen [30], but instead they are oblong with long cellular extensions, very similar to fibroblasts [31,32]. This chondrocyte phenotype is described in the literature as dedifferentiated and fibroblastic and it is accompanied by a changed protein expression as well (reviewed by Ref. [4]). Because of these differences, we speculated that DIF does not fit into the notion of a linear progression from SS to BC and then DIF. We, therefore, expected major differences also to arise at the biomarker level, especially between BC and DIF (Hypothesis III).

2. Materials and methods

2.1. Cartilage harvest

Tissue was obtained after informed consent from the distal femoral cuts of the femoral condyles from patients undergoing total knee arthroplasty for end-stage OA of the knee in the Department of Orthopedic Surgery of the University Hospital of Tuebingen, Germany, and in the Winghofer Medicum clinic, Rottenburg a.N. Germany. Full departmental, institutional and ethical committee approval were obtained before commencement of the study (project number 674/2016BO2). Articular cartilage samples from patients with degenerative OA were used. Samples from patients with any other inflammatory pathology (e.g., rheumatoid arthritis) or with posttraumatic OA after fracture were excluded. Samples were collected from a total of 164 patients, with 96 women (median age 66 years (range 44–87)) and 68 men (median age 64 years (range 51–82)) (for sex-age distribution and frequency, see Fig. S1). In addition, healthy cartilage was collected from two young patients (aged 14 and 16) who received total knee resection due to a malignant tumour.

2.2. Histological evaluation of cartilage

Following intraoperative resection, the tissue was transported and stored at 4 °C in serum-free Dulbecco's Modified Eagle's Medium (Gibco, Life Technologies, Darmstadt, Germany) with 2 % (v/v) penicillin-streptomycin and 1.2 % (v/v) amphotericin B. For top-down view analysis, tangential sections were performed using a Leica CM3050S Cryotome (Leica Microsystems GmbH, Wetzlar, Germany) directly on the resected tissue from the femoral condyle at 35 μm thickness parallel to the articular surface.

After fixation of these sections with 4 % (v/v) formalin for 30 min at room temperature, they were pre-treated with 0.2 % (w/v) collagenase A (Sigma–Aldrich, Taufkirchen, Germany) and 0.1 % (w/v) hyaluronidase (Sigma–Aldrich) in phosphate-buffered saline (PBS) for 1 h at 37 °C, followed by three washing steps with PBS. To reduce unspecific antibody binding, sections were blocked for 30 min in 5 % (w/v) bovine serum albumin and 0.3 % (v/v) Triton X-100 in PBS. This was followed by incubation with the primary antibodies at a dilution of 1:100 in 2.5 %

(w/v) bovine serum albumin-PBS at 4 °C over-night: VEGF (rabbit anti-VEGF, P802; Thermo Fisher Scientific, Waltham, MA, USA); PECAM1 (mouse anti-PECAM-1, sc-F376764; Santa Cruz Biotechnology Inc., Dallas, TX, USA); caspase 3 (rabbit anti-caspase-3, 9664S; Cell Signaling Technology, Danvers, MA, USA); caspase 8 (rabbit anti-caspase-8, 9496T; Cell Signaling Technology); P53 (rabbit anti-P53, 9282T; Cell Signaling Technology), IL6 (rabbit anti-IL-6, GTX110527; GeneTex, Irvine, CA, USA), IL1β (rabbit anti-IL-1β, ab-2105; Abcam, Cambridge, UK), DKK1 (rabbit anti-DKK-1, ET-1610-63; HuaBio, Woburn, MA, USA); FGF23 (rabbit anti-FGF-23, orb128058; Biorbyt, Cambridge, UK); osteocalcin (rabbit anti-osteocalcin, ab-93876; Abcam); osteopontin (mouse anti-osteopontin, ab-69498; Abcam); type X collagen (rabbit anti-collagen type X, ab-58632; Abcam). All antibodies were used as specified by the manufacturers. Sections were rinsed with PBS and incubated with secondary antibodies at a dilution of 1:100 (Alexa fluor 594 goat anti-mouse IgG, ab-150116; Abcam, or Alexa fluor 594 goat anti-rabbit IgG, ab-150080; Abcam) for 2 h in complete darkness. Nuclei of the cells were stained with 4',6-diamino-2-phenyindole (DAPI) at a dilution of 1:1000. Fluorescent staining was visualised with a Carl Zeiss Axiophot fluorescence microscope (Carl Zeiss Microscopy, Jena,

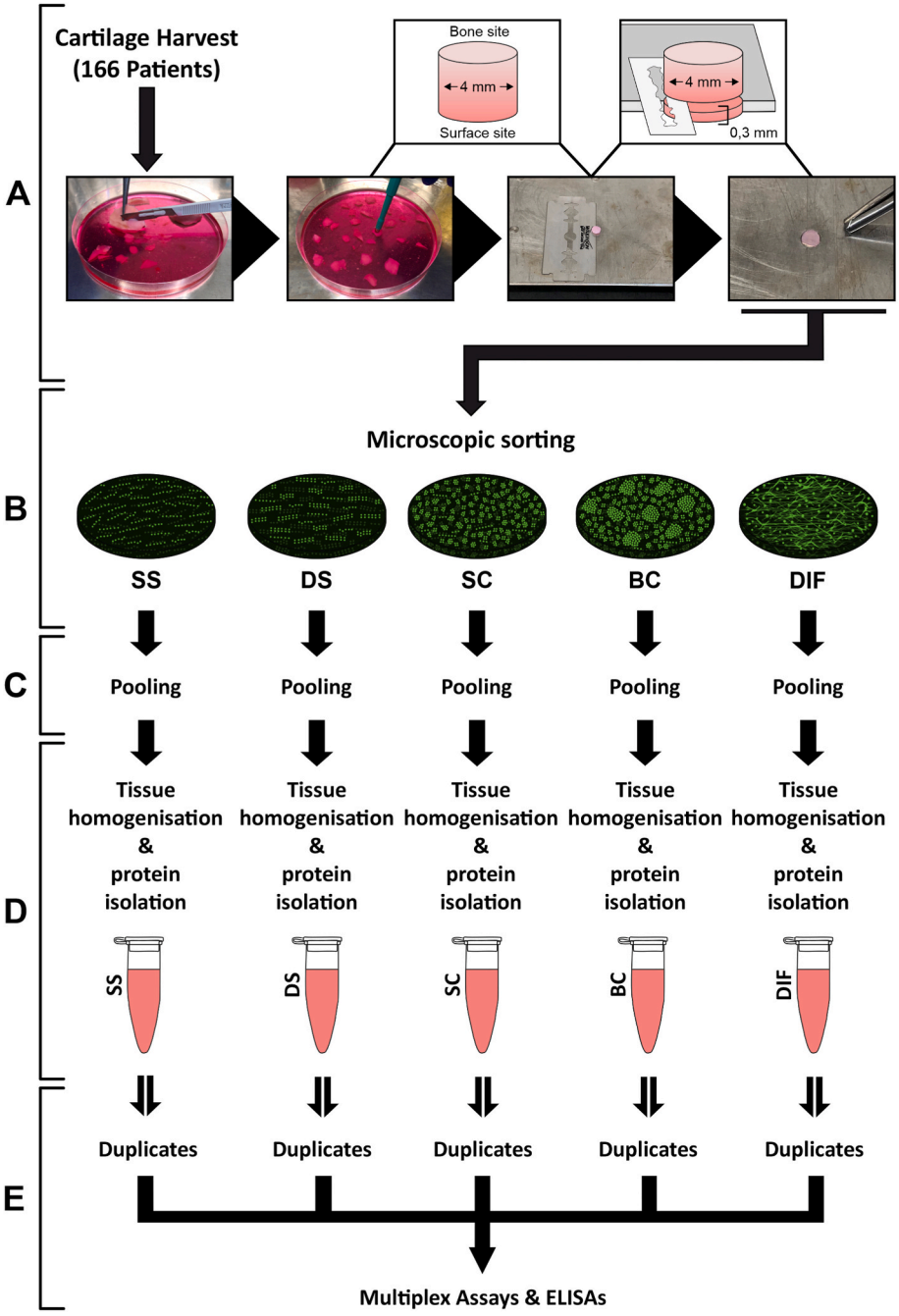

Figure 1. Flowchart of cartilage sample preparation for the quantitative biochemical analyses. Femur condyles of 164 patients undergoing total knee arthroplasty and of 2 young patients undergoing distal femur resection were collected during surgery, stored in Dulbecco's Modified Eagle's Medium (DMEM) and timely cut into 0.3 × 4 mm discs (A). Cartilage discs were then sorted by their predominant spatial cellular pattern (Single Strings (SS); Double Strings (DS), Small Clusters (SC), Big Clusters (BC) and Diffuse (DIF)) under a fluorescence microscope (B) and pooled accordingly (C). After snap-freezing, samples were stored at −80 °C. Pooled discs were homogenised in liquid nitrogen using a pestle and mortar. Proteins were then isolated and total protein content determined by means of a Bradford assay (D). Using this protein lysate, Multiplex Assays and ELISAs were then performed in duplicates (E).

Germany).

2.3. Biochemical quantification of biomarkers: multiplex assays and enzyme-linked immunosorbent assay (ELISA)

For multiplex assays, discs of articular cartilage from 41 patients and for the ELISAs discs from 125 patients (approximately 50 discs per cellular pattern category (SS, DS, SC, BC, DIF) per experiment (4 Multiplex Assays, 8 ELISAs), in total approximately 3000 discs)) were cut, sorted, and assigned to their predominant chondrocyte spatial pattern as previously described [17] (Fig. 1A–C). First, the cartilage was dissected from the bone using a scalpel no. 21 (Feather Safety Razor Co. Ltd, Osaka, Japan). From these large cartilage pieces, discs were then generated with a 4 mm biopsy punch (pfm medical ag, Cologne, Germany). Afterwards, using a custom-fabricated plate with 0,3 × 4 mm notches, the 4 mm cartilage discs were cut in the horizontal plane (i.e., in parallel to the superficial zone) to obtain round discs of 300 μm in thickness and 4 mm in diameter (Fig. 1A). These discs were then stained with 4 μM calcein-AM fluorescent dye (Cayman Chemical, Ann Arbor, MI, USA) in Dulbecco's modified Eagle's medium for 30 min at 37 °C. Calcein-stained explants were then visually classified and grouped according to their predominant cellular spatial pattern under a Leica DM IBRE fluorescence microscope (Leica Microsystems GmbH) (Fig. 1B). Pooled discs were snap-frozen with liquid nitrogen and stored at −80 °C until further use (Fig. 1C,Table S1). These frozen and grouped discs were then subjected to protein extraction through crushing them with a pestle and mortar under liquid nitrogen and then placing them on ice for 15 min in a homogenisation buffer (20 mM Tris–HCl pH 7.5, 150 mM NaCl, 1 mM Na2EDTA, 1 mM EGTA, 1 % Triton, 2.5 mM sodium pyrophosphate, 1 mM beta-glycerophosphate, 1 mM Na3VO4, 1 μg/ml leupeptin and phosphate-buffered saline 1:10; Cell Signaling Technology) added with protease inhibitors 1:200 (100 mM AEBSF, 80 μM Aprotinin, 5 mM Bestatin, 1.5 mM E−64, 2 mM Leupeptin and 1 mM Pepstatin A; Merck KGaA). The tissue homogenate was sonicated in an ultrasonic bath for 20 s and then placed on ice for 30 s. This step was repeated four times. Extracted proteins were subjected to centrifugation at 15,000g for 15 min at 4 °C, after which collection of the supernatant containing the protein phase followed (Fig. 1D). The total protein concentration across samples was determined and normalised using the Bradford protein assay (Bio-Rad Laboratories, Richmond, CA, USA). Multiplex assays and sandwich ELISAs were performed for each distinct cellular pattern (Fig. 1E). For each biomarker measured by multiplex assay (Merck KGaA, Darmstadt, Germany), a total of 33 μg of protein was used following the manufacturer's protocol. A Bio-Plex 200 System (Bio-Rad Laboratories) was used for plate read-out. The amount of total protein used for the ELISAs was as follows: 10 μg for osteocalcin (Abcam); 20 μg for type X collagen (Elabscience, Huston, TX, USA); 40 μg VEGF (Thermo Fisher Scientific); 150 μg for DKK1 (Thermo Fisher Scientific), PECAM1 (Abcam), and IL6 (Thermo Fisher Scientific); 200 μg for FGF23 (Thermo Fisher Scientific) and IL1β (Abcam); 250 μg for osteopontin (Abcam, Cambridge, UK). Absorbance was measured with an El 800 reader (BioTek Instruments GmbH, Bad Friedrichshall, Germany).

2.4. Live/dead cell assay

Discs were prepared as described above and then stained simultaneously with 4 μM calcein-AM fluorescent dye (Cayman chemical) for living cells and 2 μM propidium iodide (Thermo Fisher Scientific) for dead cells in Dulbecco's modified Eagle's medium for 30 min at 37 °C in the dark. Fluorescent staining was visualised with a Carl Zeiss Observer Z1 fluorescence microscope (Carl Zeiss Microscopy) equipped with MosaiX image acquisition software (Carl Zeiss Microscopy). Analysis was performed by counting out living and dead cells in regions of 250,000 μm^2 from acquired mosaic images of the different spatial patterns. Selection of region size was based on a previous publication [33]. For each pattern, 5 mosaic images from different patients were counted.

2.5. Statistical analysis

Values for both multiplex assays and ELISAs are presented as the arithmetic mean of two measurements (duplicate) of one pooled sample, given with the coefficient of variation as a measure of dispersion. Their graphic illustration is displayed as bar diagrams. For the live dead assay, a non-parametric analysis in the form of the median (range)/boxplot was chosen because corresponding data was not normally distributed. Experimental data for multiplex assays were acquired and calculated by Bio-Plex Manager 4.1.1 and by Microsoft Excel Version 2110 for ELISAs. Graphical illustrations (bar diagrams and boxplots) were plotted with GraphPad Prism 8.0.1.

3. Results

To quantify protein content in the tissue according to the locally predominant spatial chondrocyte pattern, multiplex assays and ELISAs were performed (Table S2 and Fig. S1). The localisation of these markers within the tissue was visualised by immunohistochemical analyses (Fig. 2 and Fig. S2).

Type X collagen, osteocalcin, and IL6 as biomarkers for hypertrophic chondrocyte differentiation showed their maximum protein levels in BC (Fig. 2C–E, and Fig. 3A, B, D). Osteopontin presented high levels from SC to DIF (Fig. 3C). Also, interleukin 8, interleukin 1β, TNF-α, and DKK1 had their highest values in BC or DIF (Table S2). The indirectly IL6-inducing leptin already had its maximum in SC, thus slightly preceding the inflammation maximum. Follistatin, HGF, and the cell-differentiation marker HBEGF presented high values in supposedly healthy SS and in the end-stage degeneration pattern DIF (Table S2).

From SS to DIF, a continuous increase in the pro-apoptotic factors JNK, BAD, and caspase 9 (Fig. 4A–C) was observed, the strongest increase thereby shown by BAD with a factor of around 15. Also, P53 and TRAIL had their highest values in DIF (Table S2). The anti-apoptotic biomarkers AKT (Fig. 4D) and BCL2 (Table S2) presented their maxima in BC and SC, respectively and decreased again in DIF. Looking at the fraction of dead cells, the live/dead cell assay indeed showed a relevant increase from DS with a median of 12 % to BC with a median dead fraction of 39 % (Fig. 4E).

Concerning angiogenesis, the pro-angiogenetic biomarkers VEGF and FGF1 (Fig. 5A and B, Table S2) increased from SS to BC while the anti-angiogenic biomarker angiopoietin 2 decreased accordingly (Fig. 5C). The angiogenic endoglin showed its maximum in DIF, and no relevant changes were observed for FGF2, PECAM1, and endothelin 1 (Table S2).

Immunomodulatory proteins were generally at a very low level with, however, a sharp increase at the transition from BC to DIF for PD1, TIM3, and TLR2 (Fig. 6). A remarkable change in biomarker levels was found from BC to DIF, where protein content either abruptly increased (TNF-α, follistatin, HGF, angiopoietin 2, PD1, TIM3, TLR2) or decreased (osteocalcin, interleukin 1β, FGF1) (Table S2).

4. Discussion

Assessing a wide range of proteins relevant in OA, we wanted to describe the dimensions of chondrocyte proliferation [1], apoptosis [2], differentiation [3,4], inflammation [5], and angiogenesis [25] in the context of local chondrocyte spatial organisation.

We hypothesised, that hypertrophic chondrocyte differentiation aggravates in the course of pattern changes from SS to BC. It had already been described that hypertrophic chondrocytes in OA cartilage occur particularly in SC and in BC, i.e., highly degenerated cartilage [30,31]. Properties of hypertrophic chondrocytes in osteoarthritic articular cartilage are thought to be similar to those in cartilage during endochondral ossification [23]. This step is characterised by destruction of the surrounding cartilage and deposition of calcium in the sense of creating a foundation for bone formation [23]. The presence of a

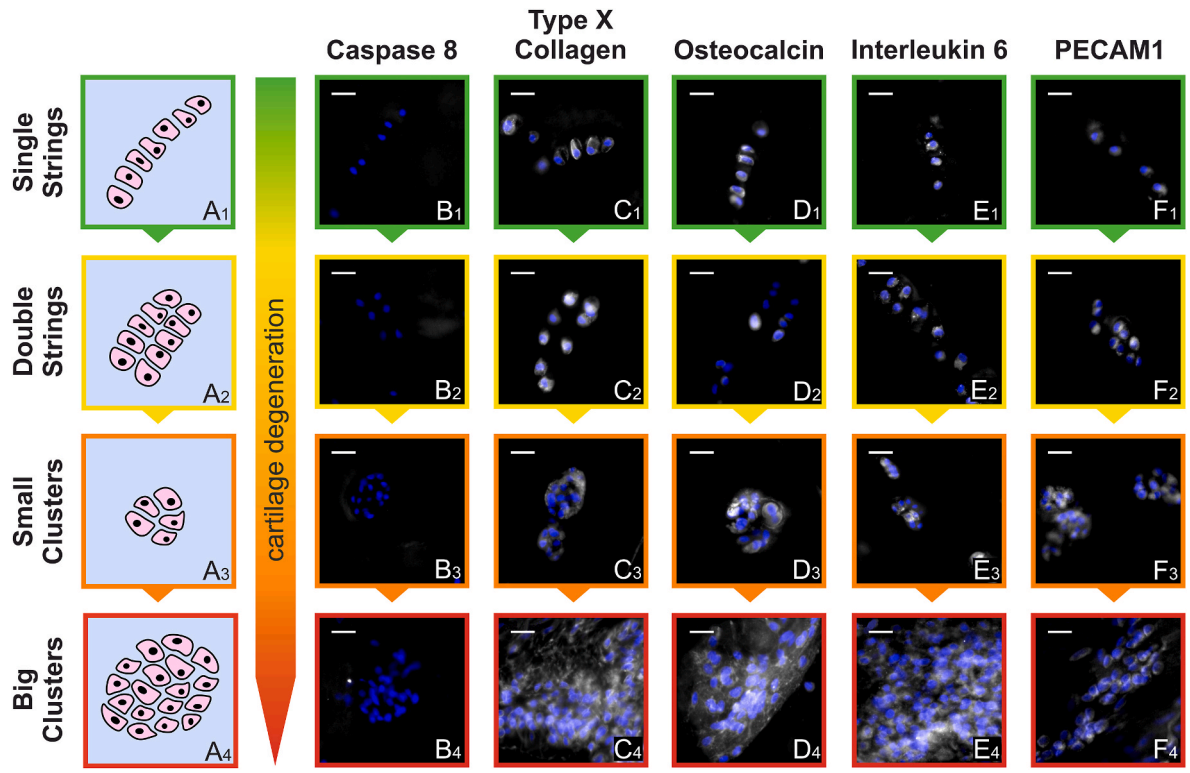

Figure 2. Signal increase in immunohistochemical analyses of inflammation and angiogenesis markers with an increasingly pathological spatial cellular pattern. Images are shown in their physiopathological order of cellular spatial organisation. A1-F1, Single Strings; A2-F2, Double Strings; A3-F3, Small Clusters; A4-F4, Big Clusters. For the apoptosis marker caspase 8 (B1-B4), no relevant signal was detected by immunolabelling. Biomarkers of hypertrophic chondrocyte differentiation such as type X collagen (C1-C4), osteocalcin (D1-D4) and interleukin 6 (E1-E4) show a clear increase in signal intensity from Single Strings to Big Clusters, especially on the extracellular side. This also applies to the angiogenesis marker PECAM1 (F1-F4). Scale bars represent 20 μm. Nuclei are stained in blue (DAPI), the stained biomarkers are visualised in white. Abbreviations: DAPI, 4′,6-diamidino-2-phenylindole, PECAM1, platelet endothelial cell adhesion molecule. (For interpretation of the references to colour in this figure legend, the reader is referred to the Web version of this article.)

hypertrophic phenotype can be recognised by the expression of proteins such as type X collagen, osteopontin, osteocalcin, and IL6. Type X collagen is predominantly produced by hypertrophic chondrocytes [34] and marks a structural change in the extracellular matrix (ECM) of articular cartilage, which is usually dominated by the presence of type II collagen [19,35]. Our results show a clear association of the amount of type X collagen with the predominating spatial chondrocyte pattern, with a high increase from DS to BC. Other markers for hypertrophic differentiation are osteopontin and osteocalcin, which are usually part of the little non-collagen organic ECM in bone. Osteopontin acts as a bridge between osteoblasts and the bone matrix. It is not only synthesised by bone cells but also by chondrocytes, in particular by hypertrophic chondrocytes [20]. It has been shown that osteopontin has inhibitory effects on matrix mineralisation in bone by activating osteoclasts and binding of calcium [36]. It has also been shown to be (possibly reactively) upregulated at sites of pathological calcification of soft tissue [37]. Osteocalcin in contrast promotes bone mineralisation. It was initially thought to be expressed by osteoblasts and odontoblasts only, but it is now established that it is also synthesised by hypertrophic chondrocytes [38,39]. Increased osteopontin and osteocalcin have even been suggested to indicate chondrocyte-to-osteoblast transformation in OA [40]. Our own results show indeed an increase in levels of osteopontin and osteocalcin as early as at the transition from SS to DS, indicating that a transformation towards the hypertrophic phenotype can be observed at already an early stage of OA. High amounts of both proteins are found in SC and BC where chondrocyte hypertrophy supposedly reaches its maximum, thus possibly leading to the cartilage-bone remodelling characteristic for OA or even post-hypertrophic osteoblast-like differentiation. Part of the increase in protein levels might be attributed to an increase in total cell number, thus not directly insinuating hypertrophic differentiation. Levels for osteocalcin, for example, increase however by a factor of 10 and drop again later in the DIF (Fig. 3), where total cell numbers are even higher. Also, collagen type X can clearly be noted extracellularly in SC and BC - a feature that cannot be observed in SS or DS (Fig. 1). Indeed, cell clusters have been identified as a distinctive histologic degenerative feature not only of OA cartilage [41], but also of intervertebral disc [42,43], meniscus [44], tendons [45], and cricoarytenoid cartilage [46]. Our findings are consistent with previous research that found that OA clusters present with a large number of proteins that are not found in normal chondrocytes [41,47-50].

IL6 was shown to activate PI3K/AKT [22]. PI3K/AKT signalling is crucial to regulate hypertrophic differentiation and proliferation of chondrocytes during endochondral ossification. Further, inhibition of PI3K/AKT leads to decreased chondrocyte hypertrophy and proliferation, resulting in reduced bone growth [51]. In both our qualitative and quantitative analysis, we found low levels of IL6 in SS, DS, and SC, but a strong increase from SC to BC, where IL6 appeared to be also relevantly present extracellularly. Taken together, all these observations strongly argue for a relevant hypertrophic differentiation in SC and, especially, BC (Hypothesis I). First changes already seem to take place at the transition from SS to DS. Next to a change in phenotype through hypertrophic differentiation, spatial pattern changes also seem to be associated with an increase in the number of cells [12,13] culminating in the formation of numerous BC [24]. In this context, the role of apoptosis has been discussed extensively in the past, and many, sometimes paradoxical, results have been reported: Sandell et al. questioned prior published apoptosis rates of up to 51 % in OA cartilage. These values would be unrealistic as in such scenarios the cartilage would entirely lose its synthesis and repair capacity. The authors suggested lower

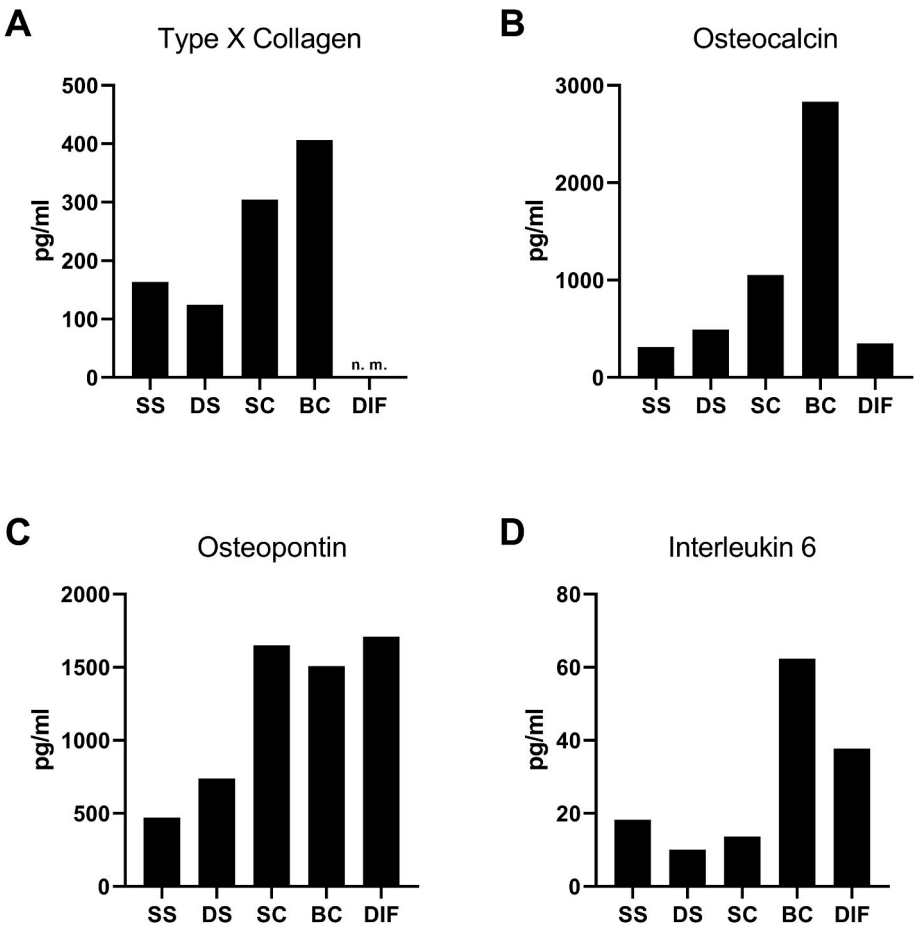

Figure 3. Markers for hypertrophic differentiation increase from Single Strings to Big Clusters. Biochemical quantification of four biomarkers of hypertrophic differentiation (type X collagen, osteocalcin, osteopontin and interleukin 6) based on the locally dominant chondrocyte pattern. Bar diagrams showing the protein content as measured by ELISA (type X collagen, osteocalcin and osteopontin) (A–C) or Multiplex Assay (interleukin 6) (D). Bars represent the arithmetic mean ($\overline{X}$) of two measurements (duplicates) of one pooled sample given in picograms per millilitre (pg/ml). For type X collagen (A), osteocalcin (B), osteopontin (C) and interleukin 6 (D), an overall increase from Single Strings to Big Clusters can be observed with an extremely prominent increase in osteocalcin. While the quantity of osteocalcin and interleukin 6 decreases from Big Clusters to Diffuse Pattern, osteopontin maintains high values from Small Clusters to the Diffuse Pattern. For type X collagen, no measurements (n. m.) were performed on the Diffuse Pattern. Abbreviations: ELISA, enzyme-linked immunosorbent assay; SS, Single Strings; DS, Double Strings; SC, Small Clusters; BC, Big Clusters; DIF, Diffuse Pattern.

apoptosis rates of around 0.1 % (unpublished data) [52].

We hence analysed also markers relevant for apoptosis and the rate of dead cells in the context of spatial chondrocyte organisation. Besides AKT, we additionally measured other key regulators of cellular proliferation and apoptosis. The levels of the pro-apoptotic markers JNK, BAD, and Caspase 9 increased from SS to DIF, while the anti-apoptotic marker AKT increased only from SS to BC. AKT is described as a powerful counter regulator of pro-apoptotic signals, particularly of pro-apoptotic members of the Bcl-2 family (e.g., BAD) [53]. Decreasing anti-apoptotic signalling by AKT from BC to DIF suggests that pro-apoptotic processes take over with DIF. In line with that, the percentage of dead cells in our live/dead assays was only around 10 % in SS and increased to almost 40 % in BC. While absolute numbers need to be handled with care due to the sensitivity of chondrocytes to undergo apoptosis in the process of tissue preparation, the increase in the rate of dead cells in BC appears highly consistent with the results from the protein level measurements.

Interestingly, in endochondral ossification, hypertrophic chondrocytes undergo apoptosis after some time and are replaced by osteoblasts [54]. This might explain why AKT reaches its highest levels in BC but decreases again with DIF. There is indeed a phenotypic resemblance of hypertrophic chondrocytes with those during endochondral ossification.

One common feature of OA and endochondral ossification is the ingrowth of vessels. Nerve fibres growing along blood vessels into the osteoarthritic cartilage from the subchondral bone are a reason for growing pain. For this vessel sprouting into cartilage, molecular signals must reach the subchondral bone [55]. We hypothesised that biomarkers of angiogenesis available in cartilage also follow specific changes along with the changes in chondrocyte spatial organisation in OA. To this end, we measured the presence of VEGF, FGF1 and Angiopoietin 2. VEGF is considered one of the main drivers of angiogenesis in OA cartilage [27]. We found VEGF to moderately increase from SS to BC. FGF1 as a ubiquitous growth factor has various effects on chondrocytes and cartilage homeostasis. It is additionally described as an inducer of endothelial cell proliferation and, therefore, angiogenesis [56,57]. FGF1 levels also steadily increased from SS to BC. The angiogenesis factor PECAM1 also showed increased levels in chondrocyte patterns associated with higher tissue degradation. Angiopoietin 2, in contrast, inhibits the growth and survival of endothelial cells by antagonising the Tie-2-receptor [58]. In our study, Angiopoietin 2 steadily decreased from SS to BC. Together these data indicate increasing induction of angiogenesis from SS to BC, thus supporting our Hypothesis II.

All these results appear conclusive in the context of a logical pattern change from SS to BC. Since cells in the DIF show a different cell morphology and pattern allocation, we hypothesised to see major

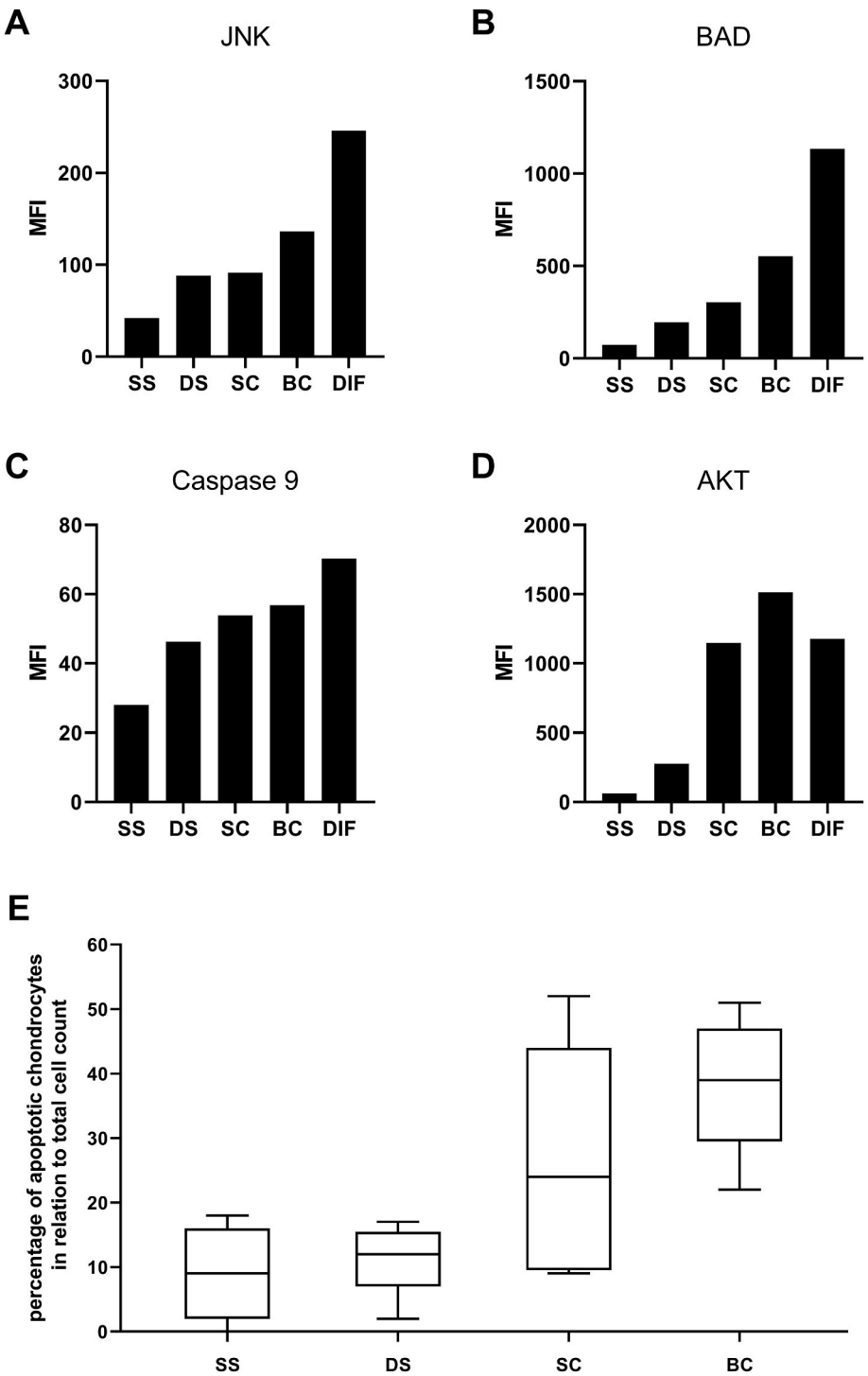

Figure 4. Apoptotic activity increases along with the spatial pattern changes in osteoarthritis. Semiquantitative biochemical analysis of biomarkers of apoptosis (JNK, BAD, Caspase 9, and AKT) (A–D) and live/dead assay (E) based on the locally dominant chondrocyte pattern. Bar diagrams showing the protein content represented in a semiquantitative fashion by median fluorescence intensity (MFI) as measured by Multiplex Assay with homogenised cartilage (A–D). Bars represent the arithmetic mean ($\overline{X}$) of two measurements (duplicates) of one pooled sample reported as the MFI. From Single Strings to the Diffuse Pattern, an increase in the pro-apoptotic markers JNK (A), BAD (B) and Caspase 9 (C) is displayed. A similar tendency can be seen in anti-apoptotic marker AKT (D) where values slightly decrease again from Big Clusters to Diffuse Pattern. (E) Boxplot showing a proportional increase of dead cells from Single Strings to Big Clusters. Live/dead assay was performed using propidium iodide (dead cells) and calcein (living cells) staining. Abbreviations: JNK, JUN N-terminal kinase; BAD, BCL2 associated agonist of cell death; AKT, Serine/threonine-protein kinase; SS, Single Strings; DS, Double Strings; SC, Small Clusters; BC, Big Clusters; DIF, Diffuse Pattern.

differences at the transition from BC to DIF (Hypothesis III). And indeed, total protein levels either abruptly increased (TNF-α, follistatin, HGF, angiopoietin 2, PD1, TIM3, TLR2) or decreased (osteocalcin, interleukin 1β, FGF1) with mostly an inversion of the prior tendency of the protein content to decrease or increase. While tissue with BC thus seems to match the described expression profile of hypertrophic differentiation (e.g. high levels of osteocalcin and IL6), this profile is very different in tissue with DIF. A large difference in biomarker levels between BC and

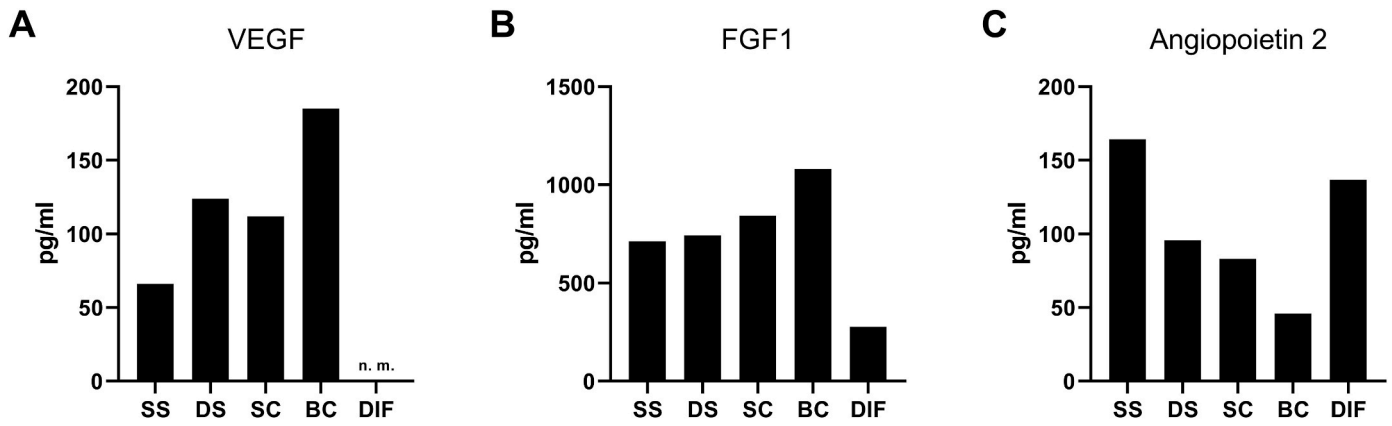

Figure 5. Angiogenesis increases from Single Strings to Big Clusters. Biochemical quantification of three prominent biomarkers of angiogenesis (VEGF, FGF1, and angiopoietin 2) was performed according to the locally dominant chondrocyte pattern. Bar diagrams showing the protein content as measured by ELISA (VEGF) (A) or Multiplex Assay (FGF1 and angiopoietin 2) (B, C) on homogenised cartilage. Bars represent the arithmetic mean ($\overline{X}$) of two measurements (duplicates) of one pooled sample given in picograms per millilitre (pg/ml). From Single Strings to Big Clusters, an increase in the pro-angiogenetic markers VEGF (A) and FGF1 (B) is shown. In accordance, a clear decrease from Single Strings to Big Clusters in the anti-angiogenetic factor angiopoietin 2 (C) can be observed. In both markers, FGF1 and angiopoietin 2, an inversion in presence can be seen from Big Clusters to Diffuse Pattern. For VEGF, no measurements (n. m.) were performed on the Diffuse Pattern. Abbreviations: VEGF, vascular endothelial growth factor; FGF1, fibroblast growth factor 1; ELISA, enzyme-linked immunosorbent assay; SS, Single Strings; DS, Double Strings; SC, Small Clusters; BC, Big Clusters; DIF, Diffuse Pattern.

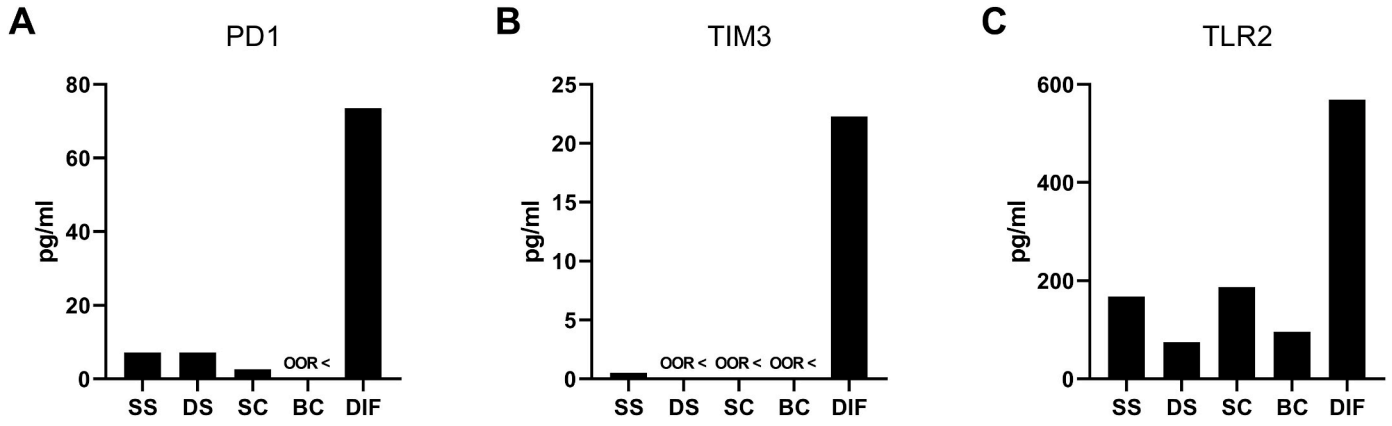

Figure 6. Immune checkpoints are exceedingly increased with the Diffuse Pattern. Biochemical quantification of three immune checkpoints (PD1, TIM3 and TLR2) analysed according to the locally dominant chondrocyte pattern. Bar diagrams showing the protein content as measured by Multiplex Assay (PD1, TIM3, and TLR2) (A, B, C) on homogenised cartilage. Bars represent the arithmetic mean ($\overline{X}$) of two measurements (duplicates) of one pooled sample given in picograms per millilitre (pg/ml). PD1 (A), TIM3 (B), and TLR2 (C) show a sharp increase at the transition from Big Clusters to the Diffuse Pattern while values from Single Strings to Big Clusters are generally at a very low level. Values under the detection limit of the Multiplex Assay are labelled as "out of range, below" (OOR <). Abbreviations: PD1, programmed cell death protein 1; TIM3, T-cell immunoglobulin and mucin-domain containing-3; TLR2, Toll-like receptor 2; SS, Single Strings; DS, Double Strings; SC, Small Clusters; BC, Big Clusters; DIF, Diffuse Pattern.

DIF also applies for markers for angiogenesis (FGF1, Angiopoietin 2). These findings support our speculation that DIF does not fit into the notion of a linear progression from SS to BC. The biomarker profile of tissue with DIF rather matches the expression profile of a dedifferentiated fibroblastic phenotype that can be identified by other markers: TNF-α promotes chondrocyte dedifferentiation [4] and Endoglin was shown to be increased in the fibroblastic phenotype [59]. Both markers were found to be highest in DIF in our data. Although extensive insights in immune response on cartilage lesions have been gained in the past [29], it remains unclear whether actual infiltration of immunomodulatory cells in articular cartilage occurs. High presence of immune checkpoints (PD1, TIM3, TLR2) and inflammatory factors (e.g. TNF-α) as well as remarkable changes in cellular morphology on DIF might support the latter fact. Especially because PD1, TIM3 and TLR2 are surface receptors that are known to be exclusively expressed on immune cells. Substantial migration or movement of cells trough the tight ECM has not been described, even though an anchoring of thin cellular extensions would at least be conceivable for superficial lesions. However, previous research stated almost no presence of immune cells in articular cartilage [60].

In addition, IL1β can also promote chondrocyte dedifferentiation and is already at a maximum at BC [61]. This fibroblastic chondrocyte phenotype appears to be a sign of a fibrocartilaginous state [18] which marks a transition from cartilage to scar tissue. Increased chondrocyte dedifferentiation could explain the low stimulus of angiogenesis of FGF1 and Angiopoietin 2 on DIF, as in healing wounds, vascularisation increases dramatically in the beginning, but decreases again to a physiological level when the scar tissue is formed [62]. This different cell profile raises the question of what role the diffuse distribution of fibroblastic chondrocytes plays in the context of osteoarthritis and in what order hypertrophic and fibroblastic chondrocytes are formed. Does this phenotype still form as a pathophysiological follow-up after BC derived from the hypertrophic chondrocytes or do we see the presence of a different cell population here? Current literature suggests that

different phenotypes coexist and that fibroblastic chondrocytes represent a dedifferentiation back to a primitive stem cell phenotype [4]. Besides the dedifferentiated fibroblastic phenotype and the terminally differentiated hypertrophic phenotype, recent findings suggested even the presence of a total of 7 molecularly defined populations of chondrocytes by single-cell RNA-sequence analysis [63].

Apart from the biomarkers that were presented in this study, there are numerous other factors having been described to play a role in the pathophysiological processes of osteoarthritis. Some of these factors or their inhibitors have already been tested in clinical trials as summarised by Zhang et al. [64]. Of high interest might be FGF-18 and its human recombinant sprifermin which was reported to increase cartilage thickness of the femorotibial joint in humans after intraarticular injection with an acceptable safety profile [65]. TGF-β, as another key regulator in differentiation processes, plays a dual role: on the one hand it positively affects articular cartilage by maintaining the differentiated chondrocyte phenotype and also stimulating chondrogenesis of precursor cells in a healthy joint, on the other hand it acts as a promoter of synovial inflammation in OA joints [23]. Inhibition of TGF-β Type I receptor protected, however, against OA degeneration in an anterior cruciate ligament transection osteoarthritis mouse model [66]. In addition, TGF-β was described to play a crucial role in arthrofibrosis for which reason its inhibition is subject of several clinical trials [67]. Investigation of IL-1 demonstrates that seemingly obvious harmful effects on chondrocytes and cartilage in vitro do not necessarily reflect in vivo: clinical trials with intra-articular injection of IL-1 inhibitors on OA patients did not lead to clinical improvement [68,69]. IL-1β was shown to promote proliferation and disorganisation of chondrocytes in growth plates of rats [70]. Our results show the highest occurrence of IL-1β in BC where the chondrocyte count per cartilage volume is the highest [12].

From the exploratory data in this study, it would seem that the pathophysiological changes of the chondrodytes stretch from SS to BC. At the transition from BC to DIF, a seemingly new phenotype is present. Investigating various biomarkers on human in-situ explants allowed us to draw observations on associations between tissue biomarker profile and cellular arrangement. This approach closes the gap between in vitro and in vivo studies and as such, stretches a big step towards translation of the observed findings. The direct association between tissue biomarker profile and cellular arrangements representing different states of OA sheds new light on the molecular and cellular physiopathology, especially in the context of larger processes such as angiogenesis, cellular proliferation, differentiation, and apoptosis. This also opens an interesting perspective for future investigation of such biomarkers and processes in clinical studies. The technical requirements to carry out such studies are already available: Tschaikowsky et al., for example, were already able to identify the differenc chondrocyte patterns by confocal laser-endomicroscopy [71], a technique that can be also carried out in the operation theatre. It should therefore be noted that next to insights on connections between macroscopic and microscopic physiopathology, now the connection between microscopic and molecular physiopathology can be better understood.

4.1. Study limitations

The main strength of the present study is the fact, that data can be provided for specific chondrocyte patterns which can be considered as having also a specific metabolic state. The price for such a selective data generation creates at the same time the main limitation of the present study, which is the need for pooling of cartilage samples. Very strict sampling to create tissue batches composed of single cellular patterns made it impossible to measure, for example, biomarkers of individual patients because of the very limited sample volume. This problem is aggravated even more in the patterns of lower cartilage degeneration, especially the supposedly healthy SS. The reason lays at hand, since patients who undergo total knee arthroplasty are expected to have cartilage degeneration of higher degree. This results in a higher occurrence of BC and lower occurrence of SS in the collected specimens.

Moreover, during the microscopic pattern-based sorting of the cartilage discs, often several different patterns were present in one single disc, resulting in the discs being discarded. This, in many cases, resulted in only very few discs of 4 × 0.3 mm size (a very low sample volume) being available per patient per specific pattern which could be used for biomarker analyses by multiplex assay or ELISA.

As a result of the cartilage pooling, the actual sample size was one - with duplicate measurements such as to recognise possible experimental errors and to better interpret the reliability of the technique. For this reason of this sample size, no inferential statistics were performed, but rather descriptive analyses are presented. These descriptive analyses represent, however, an averaged value across dozens of patients. In a small number of cases, the coefficient of variation within the measured duplicates was above 1, which limits the accuracy of the results in these cases. It is conceivable that particle interferences during measurement occurred as a result of possible inhomogeneities of the minced tissue.

To improve the availability of discs containing SS and DS, we additionally harvested cartilage discs of two young patients (aged 14 and 16) who received total knee resection due to a malignant tumour. It has already been established in the literature that cartilage composed of SS should be considered as supposedly still microscopically healthy [72-74]. Differences within one patient between cartilage areas composed for example of SS and of BC by far exceed differences between different patients or healthy subjects. For this reason, we consider the chosen sample as not a perfect, but an acceptable reference.

As also in the supposedly healthy cartilage areas, that is SS, the persevering osteoarthritic condition of the joint will have affected the cellular expression profile. For this reason, more pathologic protein levels might have been measured in SS than would have been the case in truly healthy cartilage. Although the tissue was instantly processed, the technique of sorting the cartilage first before snap-freezing might have allowed the cells to modify their expression profile as a response to the trauma of sectioning. Despite these theoretical limitations, we still see clear changes in protein levels in identically processed cartilage samples in most investigated parameters encompassing the whole range from a continuous increase to sudden extreme rises or drops. These changes are also frequently clearly associated with changes in spatial patterns.

It must also be kept in mind that measuring proteins extracted directly from the native tissue does not allow a final statement about the origin of certain biomarkers. In addition to the actual cartilage, this leaves synovia, synovial fluid, and subchondral bone as a possible origin for measured biomarkers. Many of the measured proteins were, however, structural proteins of the ECM where this phenomenon should not be of relevance. Nevertheless, the obtained results do thus not display a causality but just an association of the observed processes. To the best of our knowledge, to date no other study has used such a broad protein analysis performed on in situ human cartilage explants generated from such a large patient cohort. The aspect on doing theses analyses on a pattern specific basis is completely new. We believe that the presented exploratory data allow for an averaged perspective on the present expression profile of the chondrocytes in the different spatial chondrocyte patterns present in the development and course of osteoarthritis.

5. Conclusions

The results of our study suggest that changes in spatial chondrocyte organisation are also associated with changes in chondrocyte differentiation. Markers like type X collagen, osteopontin, osteocalcin, and its promoter IL6 showed their first relevant changes already at the transition from SS to DS. Until the formation of BC, the changes in chondrocyte differentiation are accompanied by increasing induction of angiogenesis. Drastic changes can be observed in the biomarker profile at the transition from BC to DIF. This abrupt marker change insinuates that it is either a different cell population responsible for this latter pattern or at least a different form of chondrocyte morphology.

Author contributions

JMW performed the multiplex assays and wrote the manuscript; LCG performed the immunohistochemical analyses and ELISAs, helped to interpret the data and critically revised the manuscript; SHF performed the live-dead assays and helped with the ELISAs and critically revised the manuscript; MS provided the cartilage samples, helped to interpret the data, and critically revised the manuscript; FCB supervised the experiments and helped to interpret the data; MF performed the statistical analyses and critically revised the manuscript; MD supervised the study, co-designed the study and critically revised the manuscript; UKH designed the study and wrote the manuscript. All authors read and approved the final manuscript.

Funding

Deutsche Arthrose-Hilfe e.V., Grant/Award Number: P472-A282-Wülker-EP13-hofm3-allgemein-pr–9k-2019-21.

Institutional Ethics Committee Statement: The study was conducted in accordance with the Declaration of Helsinki, and approved by the Ethics Committee of the university of Tuebingen (protocol code 674/2016BO2).

Conflicts of interest

The authors declare no conflict of interest.

Informed consent statement

Informed consent was obtained from all subjects involved in the study.

Data availability statement

All calculated data are presented. Original data are made available on reasonable request.

Authorship

All persons who meet authorship criteria are listed as authors, and all authors certify that they have participated sufficiently in the work to take public responsibility for the content, including participation in the concept, design, analysis, writing, or revision of the manuscript. Each author certifies that this material or part thereof has not been published in another journal, that it is not currently submitted elsewhere, and that it will not be submitted elsewhere until a final decision regarding publication of the manuscript in Journal of Orthopaedic Translation has been made.

Category 1

Conception and design of study: M Danalache, UK Hofmann

Acquisition of data: JM Wolfgart, LC Grötzner, S Hemayatkar-Fink

Analysis and/or interpretation of data: JM Wolfgart, FC Bonnaire, S Hemayatkar-Fink, M Schwitalle, M Feierabend.

Category 2

Drafting the manuscript: JM Wolfgart, LC Grötzner, FC Bonnaire, S Hemayatkar-Fink

Revising the manuscript critically for important intellectual content: JM Wolfgart, LC Grötzner, S Hemayatkar-Fink, M Schwitalle, FC Bonnaire, M Feierabend, M Danalache, UK Hofmann.

Category 3

Approval of the version of the manuscript to be published (the names of all authors must be listed):

JM Wolfgart, LC Grötzner, S Hemayatkar-Fink, M Schwitalle, FC Bonnaire, M Feierabend, M Danalache, UK Hofmann.

Acknowledgements

All persons who have made substantial contributions to the work reported in the manuscript (e.g., technical help, writing and editing assistance, general support), but who do not meet the criteria for authorship, are named in the Acknowledgements and have given us their written permission to be named. If we have not included an Acknowledgements, then that indicates that we have not received substantial contributions from non-authors. We thank the orthopaedic surgeons from the Department of Orthopaedic Surgery of the University Hospital of Tuebingen and from Winghofer-Medicum/Rottenburg for providing the tissue samples and the Kinderklinik Tuebingen for logistic support. We also thank the nonprofit research foundation "Deutsche Arthrose-Hilfe e.V.," Germany, for supporting this study.

Article Processing Charge

The corresponding author agrees to pay the Journal of Orthopaedic Translation Article Processing Charge upon acceptance of the work for publication in Journal of Orthopaedic Translation, unless prior arrangements have been made to waive the Article Processing Charge.

Conflicts of interest

A conflict of interest occurs when an individual's objectivity is potentially compromised by a desire for financial gain, prominence, professional advancement or a successful outcome. The Editors of the *Journal of Orthopaedic Translation* strive to ensure that what is published in the Journal is as balanced, objective and evidence-based as possible. Since it can be difficult to distinguish between an actual conflict of interest and a perceived conflict of interest, the Journal requires authors to disclose all and any potential conflicts of interest.

Section I

The authors whose names are listed immediately below certify that they have NO affiliations with or involvement in any organization or entity with any financial interest (such as honoraria; educational grants; participation in speakers' bureaus; membership, employment, consultancies, stock ownership, or other equity interest; and expert testimony or patent-licensing arrangements), or non-financial interest (such as personal or professional relationships, affiliations, knowledge or beliefs) in the subject matter or materials discussed in this manuscript.

Section II

The authors whose names are listed immediately below report the following details of affiliation or involvement in an organization or entity with a financial or non-financial interest in the subject matter or materials discussed in this manuscript. Please specify the nature of the conflict on a separate sheet of paper if the space below is inadequate.

Author names and details of the conflict(s) of interest

This Authorship & Conflicts of Interest Statement is signed by all the authors listed in the manuscript to indicate agreement that the above information is true and correct (a photocopy of this form may be used if there are more than 10 authors).

Declaration of AI and AI-assisted technologies in the writing process

The authors confirm that no AI and AI-assisted technologies were used in the writing process.

Appendix A. Supplementary data

Supplementary data to this article can be found online at https://doi.org/10.1016/j.jot.2024.08.006.

References

[1] Rothwell AG, Bentley G. Chondrocyte multiplication in osteoarthritic articular cartilage. The Journal of Bone & Joint Surgery British 1973;55(3):588–94.
[2] Del Carlo Jr M, Loeser RF. Cell death in osteoarthritis. Curr Rheumatol Rep 2008;10(1):37–42.
[3] Dreier R. Hypertrophic differentiation of chondrocytes in osteoarthritis: the developmental aspect of degenerative joint disorders. Arthritis Res Ther 2010;12:1–11.
[4] Charlier E, Deroyer C, Ciregia F, Malaise O, Neuville S, Plener Z, et al. Chondrocyte dedifferentiation and osteoarthritis (OA). Biochem Pharmacol 2019;165:49–65.
[5] Goldring MB, Otero M. Inflammation in osteoarthritis. Curr Opin Rheumatol 2011;23(5):471–8.
[6] Walsh DA, Bonnet C, Turner E, Wilson D, Situ M, McWilliams D. Angiogenesis in the synovium and at the osteochondral junction in osteoarthritis. Osteoarthritis Cartilage 2007;15(7):743–51.
[7] Kellgren JH, Lawrence J. Radiological assessment of osteo-arthrosis. Ann Rheum Dis 1957;16(4):494–502.
[8] Outerbridge R. The etiology of chondromalacia patellae. The Journal of Bone & Joint Surgery British 1961;43(4):752–7.
[9] Pritzker KP, Gay S, Jimenez S, Ostergaard K, Pelletier J-P, Revell P, et al. Osteoarthritis cartilage histopathology: grading and staging. Osteoarthritis Cartilage 2006;14(1):13–29.
[10] Rolauffs B, Rothdiener M, Bahrs C, Badke A, Weise K, Kuettner KE, et al. Onset of preclinical osteoarthritis: the angular spatial organization permits early diagnosis. Arthritis Rheum 2011;63(6):1637–47.
[11] Felka T, Zouhair S, Bast S, Struck K, Handl L, Votteler M, et al. The spatial organisation and the pericellular matrix of human foetal chondrocytes are not inborn but instead acquired characteristics. Bone & Joint Journal, Orthopaedic Proceedings Supplement 2014;96-B(SUPP_11):323. 323.
[12] Danalache M, Beutler KR, Rolauffs B, Wolfgart JM, Bonnaire FC, Fischer S, et al. Exploration of changes in spatial chondrocyte organisation in human osteoarthritic cartilage by means of 3D imaging. Sci Rep 2021;11(1):9783.
[13] Danalache M, Erler AL, Wolfgart JM, Schwitalle M, Hofmann UK. Biochemical changes of the pericellular matrix and spatial chondrocyte organization—two highly interconnected hallmarks of osteoarthritis. J Orthop Res 2020;38(10):2170–80.
[14] Felka T, Rothdiener M, Bast S, Uynuk-Ool T, Zouhair S, Ochs BG, et al. Loss of spatial organization and destruction of the pericellular matrix in early osteoarthritis in vivo and in a novel in vitro methodology. Osteoarthritis Cartilage 2016;24(7):1200–9.
[15] Tschaikowsky M, Selig M, Brander S, Balzer BN, Hugel T, Rolauffs B. Proof-of-concept for the detection of early osteoarthritis pathology by clinically applicable endomicroscopy and quantitative AI-supported optical biopsy. Osteoarthritis Cartilage 2021;29(2):269–79.
[16] Danalache M, Jacobi LF, Schwitalle M, Hofmann UK. Assessment of biomechanical properties of the extracellular and pericellular matrix and their interconnection throughout the course of osteoarthritis. J Biomech 2019;97:109409.
[17] Danalache M, Kleinert R, Schneider J, Erler A, Schwitalle M, Riester R, et al. Changes in stiffness and biochemical composition of the pericellular matrix as a function of spatial chondrocyte organisation in osteoarthritic cartilage. Osteoarthritis Cartilage 2019;27(5):823–32.
[18] Rim YA, Nam Y, Ju JH. The role of chondrocyte hypertrophy and senescence in osteoarthritis initiation and progression. Int J Mol Sci 2020;21(7):2358.
[19] Gu J, Lu Y, Li F, Qiao L, Wang Q, Li N, et al. Identification and characterization of the novel Col10a1 regulatory mechanism during chondrocyte hypertrophic differentiation. Cell Death Dis 2014;5(10). 1469-e69.
[20] Gerstenfeld L, Shapiro F. Expression of bone-specific genes by hypertrophic chondrocytes: implications of the complex functions of the hypertrophic chondrocyte during endochondral bone development. J Cell Biochem 1996;62(1):1–9.
[21] Kita K, Kimura T, Nakamura N, Yoshikawa H, Nakano T. PI3K/Akt signaling as a key regulatory pathway for chondrocyte terminal differentiation. Gene Cell 2008;13(8):839–50.
[22] Wiegertjes R, van de Loo FA, Blaney Davidson EN. A roadmap to target interleukin-6 in osteoarthritis. Rheumatology 2020;59(10):2681–94.
[23] Van Der Kraan PM. Differential role of transforming growth factor-beta in an osteoarthritic or a healthy joint. Journal of bone metabolism 2018;25(2):65.
[24] Rolauffs B, Williams JM, Aurich M, Grodzinsky AJ, Kuettner KE, Cole AA. Proliferative remodeling of the spatial organization of human superficial chondrocytes distant from focal early osteoarthritis. Arthritis Rheum: Official Journal of the American College of Rheumatology 2010;62(2):489–98.
[25] Brown R, Weiss J. Neovascularisation and its role in the osteoarthritic process. Ann Rheum Dis 1988;47(11):881–5.
[26] Mapp PI, Walsh DA. Mechanisms and targets of angiogenesis and nerve growth in osteoarthritis. Nat Rev Rheumatol 2012;8(7):390–8.
[27] Enomoto H, Inoki I, Komiya K, Shiomi T, Ikeda E, Obata K-i, et al. Vascular endothelial growth factor isoforms and their receptors are expressed in human osteoarthritic cartilage. Am J Pathol 2003;162(1):171–81.
[28] Rolauffs B, Williams JM, Grodzinsky AJ, Kuettner KE, Cole AA. Distinct horizontal patterns in the spatial organization of superficial zone chondrocytes of human joints. J Struct Biol 2008;162(2):335–44.
[29] Li M, Yin H, Yan Z, Li H, Wu J, Wang Y, et al. The immune microenvironment in cartilage injury and repair. Acta Biomater 2022;140:23–42.
[30] Hall AC. The role of chondrocyte morphology and volume in controlling phenotype—implications for osteoarthritis, cartilage repair, and cartilage engineering. Curr Rheumatol Rep 2019;21:1–13.
[31] Karim A, Amin AK, Hall AC. The clustering and morphology of chondrocytes in normal and mildly degenerate human femoral head cartilage studied by confocal laser scanning microscopy. J Anat 2018;232(4):686–98.
[32] Bush PG, Hall AC. The volume and morphology of chondrocytes within non-degenerate and degenerate human articular cartilage. Osteoarthritis Cartilage 2003;11(4):242–51.
[33] Bonnaire FC, Danalache M, Sigwart VA, Breuer W, Rolauffs B, Hofmann UK. The intervertebral disc from embryonic development to disc degeneration: insights into spatial cellular organization. Spine J 2021;21(8):1387–98.
[34] Shapiro F, Shapiro F. Developmental bone biology. Pediatric orthopedic deformities, volume 1: pathobiology and treatment of dysplasias, physeal fractures, length discrepancies, and epiphyseal and joint disorders. 2016. p. 1–158.
[35] Poole A, Kobayashi M, Yasuda T, Laverty S, Mwale F, Kojima T, et al. Type II collagen degradation and its regulation in articular cartilage in osteoarthritis. Ann Rheum Dis 2002;61(suppl 2):ii78–81.
[36] Giachelli CM, Steitz S. Osteopontin: a versatile regulator of inflammation and biomineralization. Matrix Biol 2000;19(7):615–22.
[37] Steitz SA, Speer MY, McKee MD, Liaw L, Almeida M, Yang H, et al. Osteopontin inhibits mineral deposition and promotes regression of ectopic calcification. Am J Pathol 2002;161(6):2035–46.
[38] McKee M, Glimcher M, Nanci A. High-resolution immunolocalization of osteopontin and osteocalcin in bone and cartilage during endochondral ossification in the chicken tibia. Anat Rec 1992;234(4):479–92.
[39] Pullig O, Weseloh G, Ronneberger D-L, Käkönen S-M, Swoboda B. Chondrocyte differentiation in human osteoarthritis: expression of osteocalcin in normal and osteoarthritic cartilage and bone. Calcif Tissue Int 2000;67:230–40.
[40] Lian J, McKee M, Todd A, Gerstenfeld LC. Induction of bone-related proteins, osteocalcin and osteopontin, and their matrix ultrastructural localization with development of chondrocyte hypertrophy in vitro. J Cell Biochem 1993;52(2):206–19.
[41] Lotz MK, Otsuki S, Grogan SP, Sah R, Terkeltaub R, D'Lima D. Cartilage cell clusters. Arthritis Rheum 2010;62(8):2206.
[42] Tolonen J, Grönblad M, Virri J, Seitsalo S, Rytömaa T, Karaharju E. Oncoprotein c-Fos and c-Jun immunopositive cells and cell clusters in herniated intervertebral disc tissue. Eur Spine J 2002;11:452–8.
[43] Sowa G, Vadalà G, Studer R, Kompel J, Iucu C, Georgescu H, et al. Characterization of intervertebral disc aging: longitudinal analysis of a rabbit model by magnetic resonance imaging, histology, and gene expression. Spine 2008;33(17):1821–8.
[44] Le Graverand MPH, Sciore P, Eggerer J, Rattner J, Vignon E, Barclay L, et al. Formation and phenotype of cell clusters in osteoarthritic meniscus. Arthritis Rheum 2001;44(8):1808–18.
[45] Benjamin M, Tyers R, Ralphs J. Age-related changes in tendon fibrocartilage. J Anat 1991;179:127.
[46] Dedivitis RA, Abrahão M, Simões MdJ, Mora OA, Cervantes O. Cricoarytenoid joint: histological changes during aging. Sao Paulo Med J 2001;119:89–90.
[47] Taniguchi N, Caramés B, Ronfani L, Ulmer U, Komiya S, Bianchi ME, et al. Aging-related loss of the chromatin protein HMGB2 in articular cartilage is linked to reduced cellularity and osteoarthritis. Proc Natl Acad Sci USA 2009;106(4):1181–6.
[48] Tetlow LC, Adlam DJ, Woolley DE. Matrix metalloproteinase and proinflammatory cytokine production by chondrocytes of human osteoarthritic cartilage: associations with degenerative changes. Arthritis Rheum 2001;44(3):585–94.
[49] Garimella R, Bi X, Camacho N, Sipe JB, Anderson HC. Primary culture of rat growth plate chondrocytes: an in vitro model of growth plate histotype, matrix vesicle biogenesis and mineralization. Bone 2004;34(6):961–70.
[50] Tetlow L, Woolley D. Histamine stimulates the proliferation of human articular chondrocytes in vitro and is expressed by chondrocytes in osteoarthritic cartilage. Ann Rheum Dis 2003;62(10):991–4.
[51] Ulici V, Hoenselaar KD, Gillespie JR, Beier F. The PI3K pathway regulates endochondral bone growth through control of hypertrophic chondrocyte differentiation. BMC Dev Biol 2008;8:1–15.
[52] Sandell LJ, Aigner T. Articular cartilage and changes in arthritis: cell biology of osteoarthritis. Arthritis Res Ther 2001;3:1–7.
[53] Yang E, Zha J, Jockel J, Boise LH, Thompson CB, Korsmeyer SJ. Bad, a heterodimeric partner for Bcl-XL and Bcl-2, displaces Bax and promotes cell death. Cell 1995;80(2):285–91.
[54] Gibson G. Active role of chondrocyte apoptosis in endochondral ossification. Microsc Res Tech 1998;43(2):191–204.

[55] Fenwick S, Gregg P, Rooney P. Osteoarthritic cartilage loses its ability to remain avascular. Osteoarthritis Cartilage 1999;7(5):441–52.
[56] Stegmann TJ. FGF-1: a human growth factor in the induction of neoangiogenesis. Expet Opin Invest Drugs 1998;7(12):2011–5.
[57] Cheng X, Wang Z, Yang J, Ma M, Lu T, Xu G, et al. Acidic fibroblast growth factor delivered intranasally induces neurogenesis and angiogenesis in rats after ischemic stroke. Neurol Res 2011;33(7):675–80.
[58] van Meurs M, Kümpers P, Ligtenberg JJ, Meertens JH, Molema G, Zijlstra JG. Bench-to-bedside review: angiopoietin signalling in critical illness–a future target? Crit Care 2009;13:1–13.
[59] Charlier E, Malaise O, Zeddou M, Neuville S, Cobraiville G, Deroyer C, et al. Restriction of spontaneous and prednisolone-induced leptin production to dedifferentiated state in human hip OA chondrocytes: role of Smad1 and β-catenin activation. Osteoarthritis Cartilage 2016;24(2):315–24.
[60] Chen Z, Ma Y, Li X, Deng Z, Zheng M, Zheng Q. The immune cell landscape in different anatomical structures of knee in osteoarthritis: a gene expression-based study. BioMed Res Int 2020;2020.
[61] Goldring M, Birkhead J, Sandell L, Kimura T, Krane S. Interleukin 1 suppresses expression of cartilage-specific types II and IX collagens and increases types I and III collagens in human chondrocytes. J Clin Invest 1988;82(6):2026–37.
[62] Eming SA, Brachvogel B, Odorisio T, Koch M. Regulation of angiogenesis: wound healing as a model. Prog Histochem Cytochem 2007;42(3):115–70.
[63] Ji Q, Zheng Y, Zhang G, Hu Y, Fan X, Hou Y, et al. Single-cell RNA-seq analysis reveals the progression of human osteoarthritis. Ann Rheum Dis 2019;78(1):100–10.
[64] Zhang W, Robertson WB, Zhao J, Chen W, Xu J. Emerging trend in the pharmacotherapy of osteoarthritis. Front Endocrinol 2019;10:428650.
[65] Hochberg M, Guermazi A, Guehring H, Aydemir A, Wax S, Fleuranceau-Morel P, et al. Efficacy and safety of intra-articular Sprifermin in symptomatic radiographic knee osteoarthritis: pre-specified analysis of 3-year data from a 5-year randomized, placebo-controlled, phase II study. Osteoarthritis Cartilage 2018;26:S26–7.
[66] Zhen G, Wen C, Jia X, Li Y, Crane JL, Mears SC, et al. Inhibition of TGF-β signaling in mesenchymal stem cells of subchondral bone attenuates osteoarthritis. Nature medicine 2013;19(6):704–12.
[67] Usher KM, Zhu S, Mavropalias G, Carrino JA, Zhao J, Xu J. Pathological mechanisms and therapeutic outlooks for arthrofibrosis. Bone research 2019;7(1):9.
[68] Chevalier X, Goupille P, Beaulieu AD, Burch FX, Bensen WG, Conrozier T, et al. Intraarticular injection of anakinra in osteoarthritis of the knee: a multicenter, randomized, double-blind, placebo-controlled study. Arthritis Rheum 2009;61(3):344–52.
[69] Cohen SB, Proudman S, Kivitz AJ, Burch FX, Donohue JP, Burstein D, et al. A randomized, double-blind study of AMG 108 (a fully human monoclonal antibody to IL-1R1) in patients with osteoarthritis of the knee. Arthritis Res Ther 2011;13(4):R125.
[70] Simsa-Maziel S, Monsonego-Ornan E. Interleukin-1β promotes proliferation and inhibits differentiation of chondrocytes through a mechanism involving down-regulation of FGFR-3 and p21. Endocrinology 2012;153(5):2296–310.
[71] Tschaikowsky M, Selig M, Brander S, Balzer BN, Hugel T, Rolauffs B. Proof-of-concept for the detection of early osteoarthritis pathology by clinically applicable endomicroscopy and quantitative AI-supported optical biopsy. Osteoarthritis Cartilage 2021;29(2):269–79.
[72] Aicher WK, Rolauffs B. The spatial organisation of joint surface chondrocytes: review of its potential roles in tissue functioning, disease and early, preclinical diagnosis of osteoarthritis. Ann Rheum Dis 2014;73(4):645–53.
[73] Rolauffs B, Williams JM, Aurich M, Grodzinsky AJ, Kuettner KE, Cole AA. Proliferative remodeling of the spatial organization of human superficial chondrocytes distant from focal early osteoarthritis. Arthritis Rheum 2010;62(2):489–98 [eng].
[74] Rolauffs B, Rothdiener M, Bahrs C, Badke A, Weise K, Kuettner KE, et al. Onset of preclinical osteoarthritis: the angular spatial organization permits early diagnosis. Arthritis Rheum 2011;63(6):1637–47.